

Figure 4: Comparison of a galactic evolution model due to Mathews and Schramm with stellar abundance data. This model supposes that the *r*- and *s*-processes occur in stars of different masses, so that a gradual change in the contribution ratio for neodymium is predicted which will compensate thorium decay for ages up to 15 Gyr. The predicted Th/Nd ratio vs. age is shown in (a) for this model and three maximum ages. In (b) is shown the prediction for the stable *r*- and *s*-process elements, europium and barium. It is clear that such simple models will always have trouble providing nearly constant Eu/Ba and at the same time constant Th/Nd, unless the total age is so short that thorium has not had time to decay substantially in even the oldest stars.

against the absence of a convincing mechanism in the traditional scenario for producing significant metallicity variations without altering the ratio of *r*- to *s*-process abundances. I suggest that all available data fit the initial spike model as well as they fit the synthesis in normal stars idea. One is then left in the amusing situation of having stars making helium, but with the vast majority of the helium around us having been produced in the Big Bang, and of supposing that although stars clearly make new elements via nuclear reactions, the majority of the heavy elements were made by some process preceding or accom-

panying the formation of the Galaxy. The short-lived radioactivities found in solar system material would then have their origins in such minor on-going synthesis as has taken place, and only a few species, such as the CNO isotopes, will have had their abundances measurably altered via stellar evolution.

What might the initial process be? A most exciting possibility has recently been proposed. Models concerning the quark-hadron phase transition in the Big Bang suggest that inhomogeneous conditions may have resulted during the epoch relevant to primordial nucleosynthesis (Applegate and Hogan, *Phys.*

Rev., **D 35**, 1151, 1985; Malaney and Fowler, preprint). In such conditions it appears possible to generate not only the light nuclei, but also to bridge the mass gap at atomic number 8, to produce heavy elements all the way up to U and Th. The very first generation of stars following the Big Bang would then have been responsible for the *s*-process elements seen in halo stars. Here is a plausible mechanism for synthesizing the *r*-process radioactivities which are used for cosmochronology in a single initial event. I for one will be following further studies of this idea with gleeful anticipation!

High Resolution CASPEC Observations of the $z = 4.11$ QSO 0000-26

J.K. WEBB, *Sterrewacht Leiden, the Netherlands, and Royal Greenwich Observatory, U.K.*

H.C. PARNELL, R.F. CARSWELL, R.G. McMAHON, M.J. IRWIN, *Institute of Astronomy, Cambridge, U.K.*

C. HAZARD, *Department of Physics and Astronomy, University of Pittsburgh, U.S.A.*

R. FERLET and A. VIDAL-MADJAR, *Institut d'Astrophysique, Paris, France*

Introduction

The QSO Q0000-26 is a newly discovered object with an emission redshift of 4.11 and a continuum magnitude at $\sim 6000 \text{ \AA}$ of around 17.5. The QSO was discovered as part of a programme to detect bright ($m(R) \leq 18.5$), high redshift

($z \geq 3.5$) QSOs using IIIa-F objective prism plate material taken with the UK 1.2-m Schmidt telescope at Siding Spring in New South Wales, Australia (Hazard and McMahon 1985). Q0000-26 was observed and confirmed as a high redshift QSO during an observing run on

the Anglo-Australian Telescope in August last year. Fortunate timing of a run immediately following on the ESO 3.6-m telescope meant that we were able to collect the high resolution data we present here only a few days after the object was discovered.

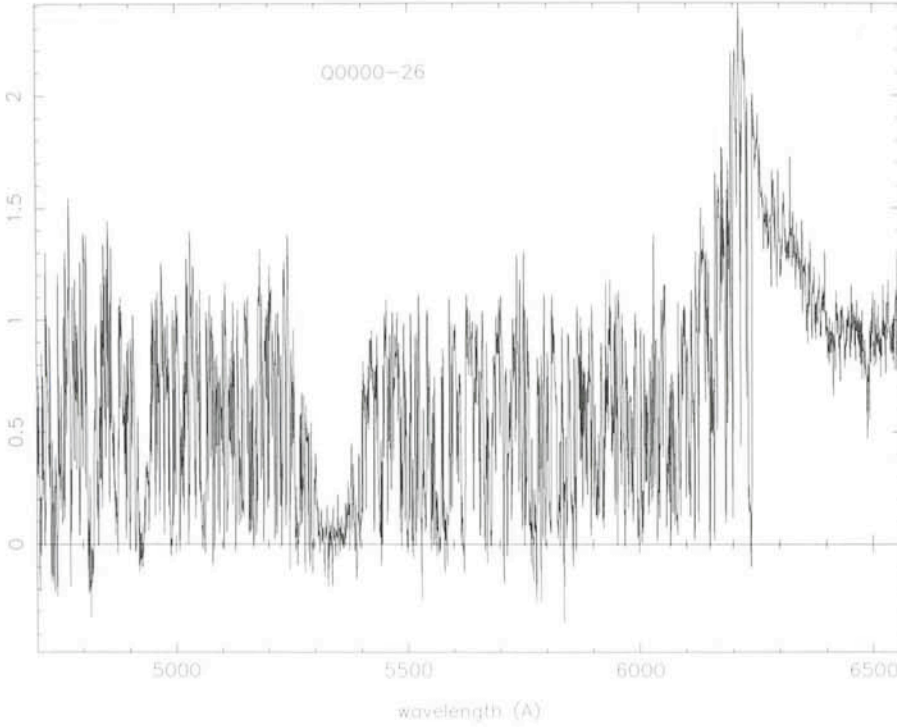


Figure 1: The spectrum of Q0000-26 obtained using CASPEC on the ESO 3.6-m telescope. The dense Ly α forest, extending right up to the Ly α emission line at 6230 Å is clearly evident.

The Observations

Q0000-26 was observed using CASPEC on the ESO 3.6-m telescope on the nights of the 30th and 31st August 1987. We used the 31.5 lines/mm grating to collect data in two overlapping wavelength regions: approximately 4700 to 5700 Å and 5600 to 6600 Å. Four 120-minute exposures were obtained for the first region and two for the second. For the lower wavelength exposures we binned the CCD (ESO # 3) by two pixels in the dispersion direction and for the higher wavelength exposures we binned by two pixels in both directions.

The slit lengths for the low and high wavelength exposures were 1,200 μm and 1,600 μm corresponding to about 8.6 and 11.5 arcsecs on the sky respectively. The slit width for all exposures was 280 μm , corresponding to about 2.0 arcsecs. This just about matched the seeing profile on our first night, when 3 out of the 4 lower wavelength exposures were obtained, and was somewhat less than the seeing on the second night, when the remaining lower wavelength and both higher wavelength exposures were obtained.

Data Reduction

Data reduction was carried out using the Starlink VAX 11/780 at the IOA in Cambridge. Cosmic rays were located either by subtracting two exposures (at the same wavelength setting) or simply

by clipping pixel values above a suitable threshold, and were then flagged. Simple median filtering, or clipping and resetting to the local mean is undesirable because of the unpredictable effect on narrow absorption lines. The two-dimensional frames were converted from ADUs to photon counts, assuming a conversion rate of 10 e⁻s/ADU. The ex-

traction of the two-dimensional data to produce spectra was then done using an optimal, seeing profile weighted procedure to maximize signal to noise in the final spectrum. Pixels containing the flagged cosmic rays were discarded and the extracted counts rescaled appropriately. An error array was generated based on Poisson statistics. Wavelength calibration was carried out in the usual way and the r.m.s. residual on arc line positions was ~ 0.05 Å corresponding to $\sim \frac{1}{6}$ of a pixel. The final spectrum was produced by adding together the calibrated orders which had been flattened by dividing by the smoothed flat field. Calibrating in this way does not produce the correct spectral shape but this does not affect our absorption line analysis. The complete spectrum thus obtained is shown in Figure 1. There was a non-uniform increased background count present in three of the lower wavelength frames, which could mean that the zero level is slightly unreliable below 5700 Å.

To determine accurately the spectral resolution, we extracted the arc spectra, adding together the individual orders in exactly the same way as the QSO spectra. By measuring the FWHM of lines in the arc spectrum, we estimate a resolution of $\sim 30 \text{ km s}^{-1}$.

The Ly α Forest

Given the high resolution of our CASPEC data, most of the absorption lines are resolved and we can use profile

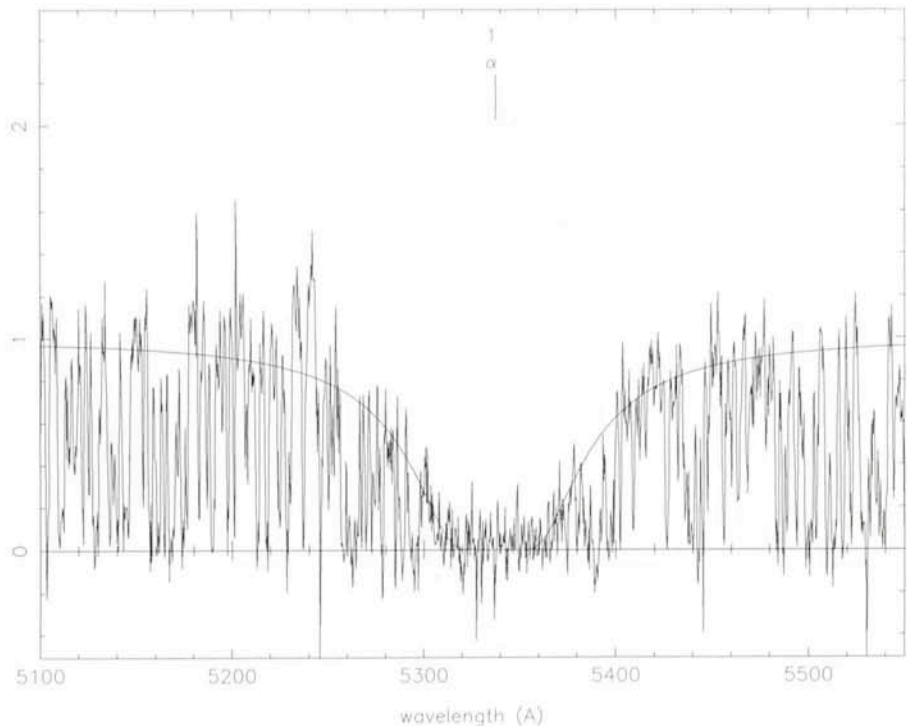


Figure 2: The spectrum in the region of the damped Ly α system at $z_{\text{abs}} = 3.392$. The smooth curve is a Voigt profile fitted to this feature with a column density of $N_{\text{H I}} = 3 \times 10^{21} \text{ cm}^{-2}$.

fitting methods to model each cloud to obtain the column density of neutral hydrogen, N_{HI} , the Doppler (velocity dispersion) parameter, b , and the redshift, z (see Carswell et al., 1987). This analysis is currently underway. Here we describe the results of a preliminary investigation of some aspects of the Ly α data.

First we fitted a single cubic spline continuum to the data using an iterative procedure which clips significant deviations below the estimated level. Clipping is carried out such that deviations in the data (excluding discarded points) about the final fit are consistent with the noise properties. The fit was done between 4700 and about 6100 Å. Over the Ly α emission line, we estimated the continuum by interpolating over regions containing absorption lines. The Ly β emission line falls immediately shortwards of a strong damped Ly α absorption line at 5340 Å and our adopted continuum will be unreliable in that region.

Next we estimated absorption line positions (centroids) and the observed equivalent widths using an automated technique (Young et al., 1979; Carswell et al., 1982) to generate a line list containing all features which deviate from the adopted continuum level by 4σ or more. Our rest equivalent width limit at this level is ~ 0.2 Å or better. Despite the extremely high number density of absorption lines, this procedure seems to work well. We checked this by comparing an expanded plot of the data with the appropriate entries in our line list.

Properties of the Ly α Forest Lines

(a) Number density evolution

As shown initially by Peterson (1978), the evolution in number of Ly α lines per unit redshift interval increases with redshift at a rate significantly faster than can be accounted for purely by cosmological effects, and consequently the clouds are evolving intrinsically. This change in the number density is well approximated by

$$\frac{dN}{dz} = N_0 (1+z)^\gamma. \quad (1)$$

We have estimated the parameters N_0 and γ from a sample of QSOs taken from the literature (Webb and Larsen; 1988), not including Q0000-26, and find $\gamma = 2.50 \pm 0.46$, and $N_0 = 2.53$ for lines with rest equivalent width, $W_{\text{rest}} > 0.36$ Å. These values agree with the estimates of Hunstead et al., 1987 for an overlapping QSO sample.

Counting lines in Q0000-26 between $z = 3.48$ (above the damped Ly α absorption and Ly β emission lines) and up to $z = 4.06$ (approximately 3,000 kms^{-1}

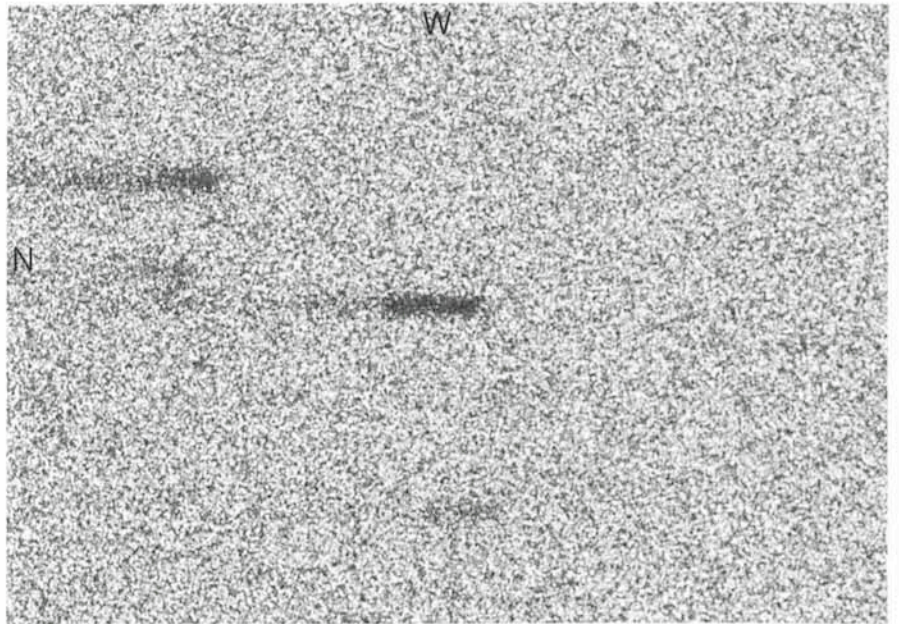
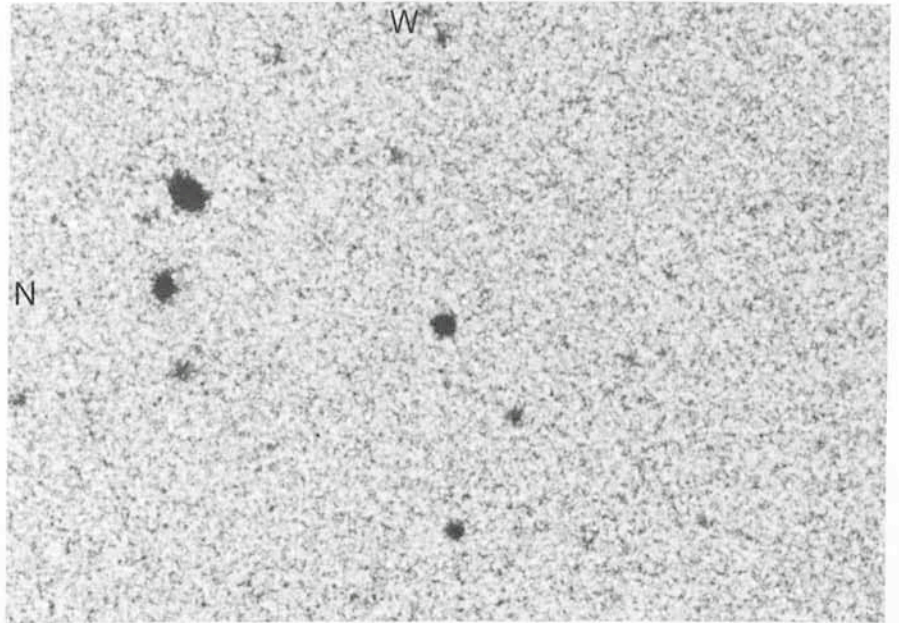


Figure 3: (a) Image of QSO0000-26 on IIIa-J+GG 395 plate for the ESO/SERC Atlas of the Southern Sky.

(b) Objective prism spectrum of QSO0000-26 on IIIa-F+GG 495 plate and 2° prism. Both plates were obtained with the UK 48" Schmidt telescope and the reproductions were made at UKSTU, Royal Observatory, Edinburgh.

below the Ly α emission line, where the local QSO ionization probably dominates) we find 68 absorption lines with $W_{\text{rest}} > 0.36$ Å. Equation (1) predicts a count of 73 and so we find that the Q0000-26 data are consistent with a continued increase in the absorption line number density up to $z \sim 4$.

(b) The Inverse Effect

When considering a single QSO, there appears to be an inconsistency in the redshift distribution of lines with equation (1); the number density is seen to increase towards lower wavelengths (Carswell et al., 1982; Murdoch et al.,

1986; Tytler, 1987; Webb and Larsen, 1988; Bajtlik et al., 1988). This is generally, although not unanimously, thought to be due to increased ionization levels for clouds in the vicinity of the QSO. In this preliminary investigation, we merely check as to whether or not such an effect is present in the spectrum of Q0000-26.

In the region $4.06 < z < 4.11$ (i.e. within 3,000 kms^{-1} of the emission redshift) we find 4 lines with $W_{\text{rest}} > 0.36$ Å compared with 7.4 predicted by equation (1). Counting lines down to our estimated 4σ limit of 0.2 Å, we find 8 lines in the same region and 164 in the range $3.48 < z < 4.06$. The ratio of these two

counts, normalized to a unit redshift interval, is 0.55 ± 0.20 and so we apparently have a significant inverse effect (at $\sim 2 \sigma$ level).

(c) *The velocity dispersion parameter*

In order to compare our data with previous analyses of high resolution data, we selected 10 apparently unblended lines in the region $3.48 < z < 4.11$. Their mean redshift was $\bar{z} = 4.0$. These lines were then modelled by using non-linear least-squares to fit Voigt profiles. For these 10 lines we find $\bar{b} = 30.5 \pm 2.1$. This can be compared with the results of Carswell et al., 1984, for Q1101-264, and Atwood et al., 1985, for Q0420-388. For Q1101-264 $\bar{b} = 30.1 \pm 2.5$ for a sample of absorption lines with $\bar{z} = 2.0$ (this is derived from the complete sample rather than just for unblended lines; the absorption line number density is sufficiently low at $z = 2$ that this should not bias the result too much) and for Q0420-388 $\bar{b} = 30.5 \pm 2.0$ for a sample with $\bar{z} = 2.9$ (for unblended lines with $\log N_{\text{HI}} > 13.75$). Our preliminary check on the Doppler parameter at $z = 4$ therefore provides no evidence for redshift evolution in this quantity.

Metal Line Systems

From this high resolution CASPEC spectrum and a low resolution (10 Å FWHM) spectrum obtained by RFC, HCP and JKW at the AAT, we have discovered two metal containing systems.

(a) $z_{\text{abs}} = 3.392$

The most prominent system is evident from the CASPEC data alone. This is

associated with the strong damped Ly α line at 5349 Å. Strong CIV absorption is seen at the same redshift in our low resolution data. Profile matching to this feature, which is probably the highest redshift candidate disk galaxy yet discovered, indicates that $N_{\text{HI}} = 3 \times 10^{21} \text{ cm}^{-2}$. The Voigt profile fitted to this feature is shown in Figure 2. At this early stage, we cannot say anything about metal abundances; many of the transitions of interest (e.g. CII λ 1334, SiII λ 1260, Si III λ 1206, SiIV $\lambda\lambda$ 1393, 1402) are embedded in the Ly α forest and a detailed profile analysis is required to obtain column densities (or limits).

(b) $z_{\text{abs}} = 4.133$

This system has a redshift 1,350 km s⁻¹ greater than the Ly α emission line, and so presumably resides in the same cluster of galaxies as the QSO itself. Strong CIV absorption is seen in the low resolution spectrum, although the hydrogen column density is not particularly high (probably less than a few times 10^{17} cm^{-2}). This feature is not seen in the high resolution data as it is outside the wavelength range. The higher order Lyman lines are present in the CASPEC data and they should provide an accurate column density estimate. Since this object evidently sits fairly close to the QSO, we might expect the gas to be highly ionized, and so we searched for OVI absorption. This is a doublet with rest frame wavelengths 1031.9 and 1037.6 Å. The 1031 line appears to be present but this is unfortunately ambiguous since the 1037 line is blended with the damped Ly α line.

We expect the full analysis of these data to take some time and that the results will supply new and valuable in-

formation on the nature of the Ly α clouds at the highest redshift so far available. Later this year, we aim to collect more CASPEC data on the spectrum of Q0000-26, covering wavelengths longward of the Ly α emission line. These will cover many of the metal line transitions associated with the two systems discovered and will enable us to study the abundances and ionization conditions at this early epoch.

References

Atwood, B., Baldwin, J.A., and Carswell, R.F., 1986, *Astrophys. J.*, **292**, 58.
 Bajtlik, S., Duncan, R.C. and Ostriker, J.P., 1988, preprint.
 Carswell, R.F., Whelan, J.A.J., Smith, M.G., Boksenberg, A., Tytler, D., 1982, *Mon. Not. R. Astr. Soc.*, **198**, 91.
 Carswell, R.F., Morton, D.C., Smith, M.C., Stockton, A.N., Turnshek, D.A., and Weymann, R.J., 1984, *Astrophys. J.*, **278**, 486.
 Carswell, R.F., Webb, J.K., Baldwin, J.A., and Atwood, B., 1987, *Astrophys. J.*, **319**, 709.
 Hazard, C. and McMahon, R.G., 1985, *Nature*, **314**, 238.
 Hunstead, R.W., Pettini, M., Blades, J.C., and Murdoch, H.S., 1987, in *IAU Symposium 124, Observational Cosmology*, ed. A. Hewitt, G. Burbidge and L.Z. Fang (D. Reidel) p. 799.
 Murdoch, H.S., Hunstead, R.W., Pettini, M., and Blades, J.C., 1986, *Astrophys. J.*, **309**, 19.
 Peterson, B.A., 1978, in *IAU Symposium 79, The Large Scale Structure of the Universe*, ed. M.S. Longair and J. Einasto (D. Reidel), p. 389.
 Tytler, D., 1987, *Astrophys. J.*, **321**, 69.
 Webb, J.K. and Larsen, I.P., 1988, to appear in proceedings of the Third IAP Astrophysics Meeting, *High Redshift and Primeval Galaxies*. (Edition Frontières)
 Young, P.J., Sargent, W.L.W., Boksenberg, A., Carswell, R.F., Whelan, J.A.J., 1979, *Astrophys. J.*, **229**, 891.

Remote Observing: Nine Days in Garching

C. WAELENS, *Astronomical Institute, University of Leuven, Belgium*

As announced by G. Raffi in the *Messenger* No. 49 and confirmed by P. François in the *Messenger* No. 50, the CES spectrograph equipped with CCD (using the CAT telescope) can now be operated by means of remote control from Garching. I had the chance to be the first visiting observer with these instruments in Garching, and was asked to write down my impressions for the readers of the *Messenger*.

Before leaving my home institute, I was warned by several colleagues who feared that remote control was an addi-

tional step toward a practice of observational astronomy where most of the romantic side of the job has gone away. My answer was that an observation run from Garching allowed me to stay a few days longer with my newly born son, and that there was some romanticism there too. I could also have replied how fascinating an experience it is to be in touch with one of the amazing technical developments at ESO. It surely is a remarkable achievement that, so early in the development of the remote control technique, observations could be

carried out from Garching with essentially the same efficiency as at La Silla, an achievement for which G. Raffi, G. Kraus, and M. Ziebell deserve to be congratulated. My warmest thanks also go to the numerous colleagues both in La Silla and in Garching who helped in rendering the operations as efficient as possible.

My programme was an easy one for remote control, since I have been using the same spectral range throughout, watching variations of the profile of the SiIII line at 4552 Å in some bright Beta